Catalysis Science & Technology

Accepted Manuscript

ROYAL SOCIETY OF CHEMISTRY

www.rsc.org/catalysis

Journal Name

ARTICLE

Steady-State Reaction Kinetics of CO Oxidation Catalyzed by Uni-Sized Pt_{30} Clusters Directly Bound to Si Surface

Received 00th January 2015,
Accepted 00th January 20xx

DOI: 10.1039/x0xx00000x

www.rsc.org/

H. Yasumatsu*[,a] and N. Fukui[b]

Catalytic activities of CO oxidation driven by uni-sized Pt clusters directly bound to a Si substrate surface, Pt_{30}/Si, are reported. The CO_2 production rate was measured as a function of the cluster temperature under steady-state conditions with continuous and simultaneous flow of CO and O_2 as well as at fixed reactant exposure followed by a temperature-programed desorption mass-spectroscopy. The highly selective, sensitive and reliable detection of the catalytic CO_2 products allows determining the CO oxidation rate against non-negligible back-ground CO_2, in spite of Pt in the catalyst sample as little as 30 ng. It was demonstrated that Pt_{30}/Si is a durable and high-performance CO-oxidation catalyst even repeating the reaction cycle in coexistence with CO and O_2 in the temperature range below 630 K. It is probable that the high performance catalytic activity originates from efficient reductive activation of oxygen by electrons enriched at the subnano-interface between Pt_{30} and the Si substrate surface.

Introduction

It is promising that enriched electrons can promote molecules to active species through reductive excitation initiated by their electron capture. Focusing on catalysis as one of the practical functions desired for solving the global key issues of energy and materials we are confronted with, numbers of research studies have been reported that catalytic activities are gained by extra electronic charges in/around supported nanoparticles.[1] Haruta and his coworkers have discovered catalytic activities of gold nanoparticles, despite the high chemical stability of bulk gold, because of extra negative charges at the periphery of the gold nanoparticles as a result of interaction with the supporting substrate.[2] For smaller clusters, it has been reported that the charging state of the gold clusters supported on an MgO(100) thin film relates closely to their catalytic activities.[3-5] High activity of CO dissociation by nickel clusters supported on the MgO(100) thin film prepared on a Mo(100) substrate is owing to size-dependent electron transfer from the cluster to anti-bonding molecular orbitals of CO adsorbed,[6] where the cluster size is defined as the number of the constituent atoms of the cluster. Distinct cluster-size dependence of the charging states of gold clusters supported on MgO/Ag(001) thin films have been explained on the basis of quantized electronic levels in a quantum well and their level closing at the magic numbers of electrons charged from the Ag support surface through the MgO films.[7] It is obvious that the cluster size is one of the most important parameters to be tuned in order to obtain the most appropriate catalytic activity for individual reactions focused on.

We have found low-temperature catalytic activity in CO oxidation driven by uni-sized Pt clusters, Pt_N (N=10–60, cluster size), directly bound to a Si semiconductor substrate[8-11] by means of Temperature-Programmed Desorption Mass-Spectroscopy (TPD-MS);[12-15] hereafter this catalyst is described as Pt_N/Si. Considering similarities between Pt_N/Si and the Pt(111) single crystal surface in the TPD spectra[12-16] and the Pt-Pt internuclear distance,[8] it was concluded that the CO oxidation takes place in accordance with the Langmuir-Hinshelwood mechanism[17] also on the Pt_N/Si catalyst. It was discovered that CO_2 is produced at as low as 120–140 and 130–350 K by catalytically-activated molecular and atomic oxygen species, respectively, adsorbed on the catalysts, the latter of which starts at 70–80 K lower than the same reaction on the Pt(111) surface.[16] This specific activity has been explained in terms of enriched electrons accumulated in a Schottky barrier junction at a sub-nano interface between Pt_N and the Si surface,[12,15] where the electron accumulation has been clearly indicated through our STM/STS (Scanning-Tunneling Microscopy/Spectroscopy) studies[10] and *ab initio* calculations.[11] Furthermore, the higher catalytic performance of Pt_{60}/Si than Pt_{30}/Si originates from the larger storage capacity of dissociatively-adsorbed oxygen as the reduction reagent.[12]

One of crucial issues in heterogeneous catalysts for gas treatments is poisoning by CO molecules, for instance,

[a] *Cluster Research Laboratory, Toyota Technological Institute: in East Tokyo Laboratory, Genesis Research Institute, Inc., 717-86 Futamata, Ichikawa, Chiba 272-0001, Japan.*
[b] *East Tokyo Laboratory, Genesis Research Institute, Inc. 717-86 Futamata, Ichikawa, Chiba 272-0001, Japan.*
* To whom correspondence should be addressed. E-mail: yasumatsu@clusterlab.jp
Electronic Supplementary Information (ESI) available: [details of any supplementary information available should be included here]. See DOI: 10.1039/x0xx00000x

covering the catalysts, which inhibit catalytic activation of oxygen. Reactivation of the catalyst needs thermal desorption of the CO poison molecules at a cold start of an automobile catalyst as one of the representative and practical examples, so that it results in increase in fuel consumption. Therefore, improvement of catalysts to gain anti-poisoning properties is strongly desired in practical application.

In this report, we describe our recent experimental studies to demonstrate substantial and durable catalytic performance of the CO oxidation driven by Pt_{30}/Si, as a representative of the Pt_N/Si catalysts, even repeating the measurements for a given catalyst under steady-state conditions with continuous supply of O_2 and CO as a reactant as well as a poison; the properties such as the thermal stability,[18] the electronic structure[10,11] and TPD of the CO oxidation[13-15] have been studied most for this size. Highly selective, sensitive and reliable mass-analysis allowed us to quantitatively detect CO_2 produced by the Pt_{30}/Si catalyst including as little as 30-ng Pt against non-negligible back-ground CO_2 produced from the residual O_2 and CO. In combination with the result of the TPD-MS, the high performance catalytic activity of the Pt_{30}/Si catalyst is discussed on the basis of the CO oxidation rate measured as functions of the catalyst temperature and the partial pressures of CO and O_2.

Experimental

Slow impact[19] of size-selected Pt_{30}^+ onto a 7×7 reconstructed Si(111) surface allows the uni-sized monatomic-layered Pt_{30} disk to stick on the Si surface[8] stably as high as 673 K in vacuum.[18] Its catalytic performance under a given steady-state reaction condition was evaluated by mass-analysing CO_2 produced by the catalyst at constant partial pressures, P_{CO} and P_{O2} (< 1×10^{-4} Pa), of CO and O_2 (Taiyo Nippon Sanso Corp. ≥99.999% pure), respectively. The isotope, ^{13}CO (SI Science Co., Ltd., >99% pure), was employed to distinguish the catalytic product, $^{13}CO_2$, from residual $^{12}CO_2$ in the vacuum chamber, although back-ground $^{13}CO_2^+$ are still formed on the electron-gun filament of the mass analyzer from the residual ^{13}CO and O_2, the contribution of which was measured independently. The details of the experimental apparatus have been reported elsewhere.[12,13,20-22]

Preparation of Pt_{30}/Si catalyst

The Pt cluster ions, Pt_N^+, were produced by sputtering of a Pt disk (Tanaka Kikinzoku Kogyo K.K. >99.99% pure) in a gas-aggregation chamber equipped with a magnetron-sputtering device,[8,20-22] and the desired cluster size of 30 was selected out by passing through a quadrupole mass filter. Reducing both their kinetic energies and ion-beam diameter in collision with He gas at 100 K,[21] the uni-sized Pt_{30}^+ were allowed to collide onto a circular area (8 mm in diameter) of the Si substrate surface, so as to bind Pt_{30} to the substrate surface,[8-11,19] at a substrate temperature, T_s, of 300 K at a collision energy of 1 eV per Pt atom and at an ambient pressure less than 5×10^{-8} Pa, most of which is due to He from the cluster-ion source and the collisional cooling device. Then, the surface was passivated with hydrogen by irradiating an atomic hydrogen beam at T_s < 350 K in order to suppress oxidation of the silicon substrate surface and hence to prevent the Pt cluster from embedding in silicon oxides; the H-terminated silicon surface is stable up to 750 K,[23] while the H atoms are desorbed from Pt_N at 450 K by analogy with supported Pt catalysts.[24] It has been confirmed that the H-terminated silicon surface without the Pt clusters does not contribute to the CO oxidation,, and this is consistent with the TPD experiments performed with this surface.[12]

The number and weight of Pt_{30} on the substrate surface was 3.1×10^{12} and 30 ng, respectively. The fraction of the cluster overlapping on the substrate was estimated to be 20%, assuming that the spatial distribution of the deposited clusters obeys Poisson (random) arrangement and that they are monatomic-layered disks with a diameter of 1.4 nm corresponding to close-packed arrangement of the Pt atoms having its metallic radius (=0.13 nm).[8] Because of this small fraction of the overlap, direct interaction between the clusters was neglected in the present study.

The Si(111)−7×7 reconstructed surface was prepared from a Si wafer (Nilaco, n-type, <0.02 Ωcm, 10×27×0.5 mm^3) by repeating more than ten sets of resistive heating at 1130 K for 50 s followed by annealing down to 850 K at a rate of -0.5 K s^{-1} at an ambient pressure less than 5×10^{-7} Pa, where the base pressure was less than 5×10^{-9} Pa. The substrate temperature was measured with a chromel-alumel thermocouple (0.1 mm in diameter) wrapped with tantalum foil (0.075-mm thick), which was sandwiched between the sample and a dummy Si substrate at the center bottom of them. The temperature uniformity on the sample surface was confirmed to be within 10 K at 850 K by measuring with a pyrometer.

Detection of products produced by Pt_{30}/Si catalyst

The $^{13}CO_2$ catalytic product was mass-analyzed, while heating resistively the substrate together with the cluster catalyst to 630 K at the rate of 0.2–0.3 K s^{-1} and at constant P_{CO} and P_{O2}. The ramping rate is sufficiently slow to consider that the temperature of the clusters is always equal to T_s, and that the measured rate was not changed in this ramping-rate range. In order to escape hysteresis in the catalysis, the Pt_N/Si catalyst was heated to 630 K at given P_{CO} and P_{O2} in prior to the catalysis measurement at these P_{CO} and P_{O2}. The mass analysis was attained by means of a quadrupole mas-filter equipped in a differentially-pumped chamber through a skimmer having a hole of 6 mm in diameter. The catalyst sample surface was placed at < 1 mm far from the skimmer in order to increase the collection efficiency of the catalytic product desorbed from the catalyst surface as well as to reduce inflows of ^{13}CO and O_2 into the electron gun.[20] This procedure increases remarkably the selectivity of the detection of CO_2 produced by the catalyst against the back-ground CO_2 produced at the electron gun; a typical ratio between the catalytic and back-ground CO_2 intensities is ~10 as shown in Figure 1 below. The reliability of the detection is secured by reproducible placing of the catalyst sample in front of the skimmer to maintain the

collection/detection efficiency of the catalytically produced CO_2 and the back-ground CO_2 intensity under a given reaction condition. The detection limit for Ar is as low as 4×10^{-12} Pa in the reaction chamber as stated in our previous report.[20] The limit for the mass analyzer itself should be in the order of 10^{-13} Pa, considering that the pressure ratio between the reaction and analyzer chambers is > 40 because of the differential pumping of the analyzer chamber. The detection efficiency of $^{13}CO_2^+$ was calibrated with Ar^+ intensity on a plausible assumption that the ratio of the transmittances of Ar^+ and $^{13}CO_2^+$ through the quadrupole mass-filter and the ion lenses, and hence that of their detection efficiencies is always the same considering the small mass-difference between them. The gas composition of Ar, ^{13}CO and O_2 were measured during all the catalysis measurements by means of a residual gas analyzer, while the total pressure a cold cathode gauge.[12]

Temperature-programmed desorption mass-spectroscopy

The procedure is the same as that reported previously.[12] Briefly, the Pt_{30}/Si catalyst was reduced by ^{13}CO at T_s=630 K within 5 min before every set of the TPD measurement. Then, O_2 or ^{13}CO was supplied one by one at a given amount of exposure for each at T_s=105 K. While heating this catalyst to 630 K at the rate of 0.3 K s^{-1}, the desorbed $^{13}CO_2$ product was mass-analyzed.

Results

Intensity of CO_2 catalytically produced under steady state condition

Panel (a) of Figure 1 shows raw data of the $^{13}CO_2^+$ intensity measured as a function of T_s in the CO oxidation catalyzed by Pt_{30}/Si at $P_{CO}=2.9\times10^{-5}$ Pa and $P_{O2}=1.0\times10^{-4}$ Pa. The standard deviation of the count rate around 28000 cps (T_s~490 K) was 229 cps, while the statistical error at 28000 cps is theoretically 306 cps, considering the time constant (0.3 s) of the counting rate meter employed. This agreement indicates sufficient reliability of the present measurements.

The contribution of the back-ground $^{13}CO_2^+$ produced at the electron gun was measured independently before and/or after a set of the catalysis measurements at a given P_{O2} by placing the Pt_{30}/Si sample, which was intentionally and completely CO-poisoned, in front of the skimmer of the mass analyzer. Panel (b) of Figure 1 shows the intensity, I_{bg}, of the back-ground $^{13}CO_2^+$ as a function of P_{CO} measured at T_s=360 K and at $P_{O2}=1.0\times10^{-4}$ Pa. The intensity, I_{bg}, increases linearly with P_{CO} as a broken line displayed in this panel, which was obtained by linear fitting;

$$I_{bg} / \text{cps} = 4.9\times10^{7}\, P_{CO} / \text{Pa} + 2.7\times10^{2} \quad (1),$$

where the intercept originates from the dark noise in the counting signal owing to exited metastable neutral species passing through the mass filter.[20] It is noted that this relation has been reproduced using a blank substrate without the Pt_N

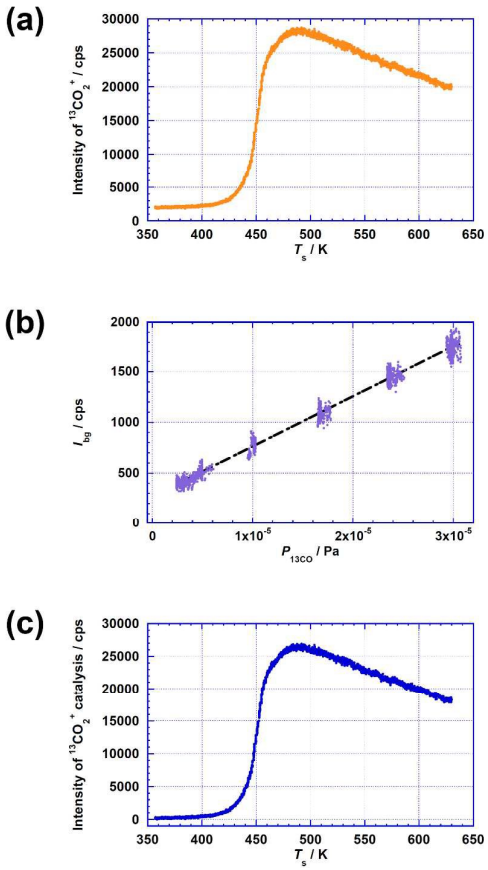

Fig. 1 (a) Raw data of $^{13}CO_2^+$ intensity measured in the CO oxidation catalyzed by Pt_{30}/Si at partial pressures of the reactant gases, ^{13}CO and O_2, of P_{CO}= 2.9×10^{-5} Pa and $P_{O2}=1.0\times10^{-4}$ Pa, respectively. (b) Intensity, I_{bg}, of back-ground $^{13}CO_2^+$ measured as a function of P_{CO} at $P_{O2}=1.0\times10^{-4}$ Pa. A result of linear fitting of the back-ground $^{13}CO_2^+$ intensity is indicated as a broken line. (c) Intensity of $^{13}CO_2^+$ originating from $^{13}CO_2$ catalytically produced in the CO oxidation by Pt_{30}/Si, which was obtained by subtracting I_{bg} according to the linear fitting shown in panel (b) from the measured $^{13}CO_2^+$ intensity shown in panel (a).

deposition instead of the completely poisoned Pt_{30}/Si irrespective of T_s in the range of 300–630 K.

Panel (c) of Figure 1 shows the intensity of $^{13}CO_2^+$ originating from $^{13}CO_2$ produced in the CO oxidation catalyzed by Pt_{30}/Si, which was obtained by subtracting I_{bg} according to eq. (1) from the $^{13}CO_2^+$ intensity shown in panel (a).

Dependence of catalytic CO oxidation rate on CO and O_2 pressures

Figure 2 shows a relative CO oxidation rate of the Pt_{30}/Si catalyst under various steady-state reaction conditions at $P_{O2}=1.0\times10^{-4}$ and 2.5×10^{-6} Pa, which was obtained on the basis of the intensity of $^{13}CO_2^+$ originating from the catalytic $^{13}CO_2$ product with considering P_{O2} dependence of the detection efficiency calibrated (difference of a factor of ~25 between the two P_{O2}); a small fluctuation (5%) in P_{O2} was smoothed with first-order dependence of the CO oxidation rate on P_{O2}.[25] At larger pressure ratio, P_{CO}/P_{O2}, the rate

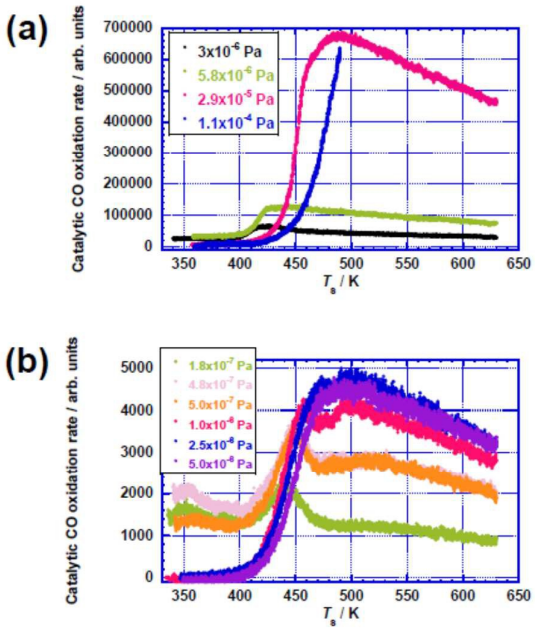

Fig. 2 Relative CO oxidation rate of the Pt_{30}/Si catalyst under steady-state reaction conditions at the partial pressure of O_2, (a) P_{O2}=1.0×10^{-4} Pa and (b) 2.5×10^{-6} Pa, and at various ones of ^{13}CO, P_{CO}, as indicated in the figure. The rates at a similar pressure ratio, P_{CO}/P_{O2}, are plotted in the same color.

changes with T_s in a manner of a so-called universal curve,[26] i.e. no CO oxidation takes place below ~380 K, the rate increases rapidly with T_s, and then decreases gradually. At smaller P_{CO}/P_{O2}, on the other hand, the CO oxidation takes place below 330 K with relatively little T_s dependence. The peak observed in the range of T_s=400–470 K at low P_{CO} as shown in panel (b) reflects relatively slow transition from CO-rich to O-rich regimes compared to the present ramping rate of T_s under these reaction conditions.[25]

Temperature-programmed desorption measurements

Figure 3 shows TPD spectra of $^{13}CO_2$ produced by the Pt_{30}/Si catalyst at the exposure amount of 10 L for each reactant, but in the different orders of the reactant exposure, where the back ground has been subtracted. When O_2 is supplied to the catalyst in prior to ^{13}CO, the TPD spectrum reproduces that reported previously;[12] two peaks are pronounced at T_s=130 and 260 K, and a broad component bridges them, tailing to ~ 400 K. As described in our previous report,[12] the peak at 130 K is assigned to the reaction between O_2 and ^{13}CO on the catalyst, while the peak at 260 K and the broad component to the CO oxidation by an ordered species of O adsorbates and a disordered one, respectively. In contract to this, no $^{13}CO_2$ is produced in the opposite order of the reactant exposure.

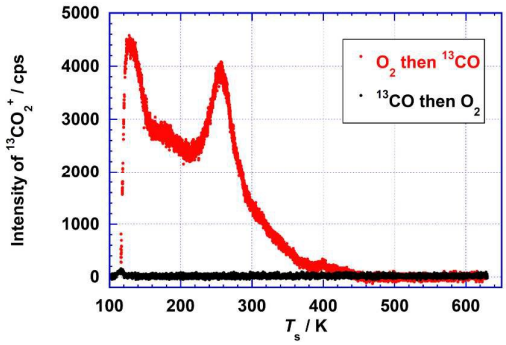

Fig. 3 TPD spectra of $^{13}CO_2$ produced by the Pt_{30}/Si catalyst at the exposure amount of 10 L for each reactant. The red circles show the $^{13}CO^+$ intensities when the catalyst was exposed to O_2 firstly, then to ^{13}CO, while the black ones in the opposite order of the reactant exposure. The back ground has been subtracted.

Discussion

All of the steady-state reaction-kinetics measurements as well as the TPD-MS ones were reproduced very well, even repeating the heating cycles with the same catalyst sample more than 100 times in a few weeks. Therefore, the Pt_{30}/Si catalyst is durable in the present reaction conditions. Furthermore, it was demonstrated that this sample acts as a catalyst, i.e. the sample returns to the same chemical state when it is put in the same environment with the same reaction procedure.

The Pt_{30}/Si catalyst starts its catalytic performance at T_s at least 50 K lower than the Pt(110) surface[27] as one of the representative active model catalysts, even considering the slight difference in the reaction condition, where this temperature reduction is in consistent with the result of the TPD-MS measurement.[12]

The T_s dependence at larger P_{CO}/P_{O2} can be explained according to the universal curve.[26] Below ~380 K, the surface of the Pt_{30}/Si catalyst is covered with CO because of both the larger gas-composition of CO and its larger sticking probability than that of O_2, so that the catalyst is completely CO-poisoned and catalytically inactive at all. As shown in Figure 3, the Pt_N/Si catalyst is completely poisoned by the CO adsorption when CO is supplied to the catalyst in prior to O_2.

With increase in T_s, the CO poisons can move off the catalyst or be desorbed at sufficiently high T_s, and the catalyst starts having room for the activation of oxygen. Once the CO oxidation starts, the CO poisons are oxidatively removed by the activated O, so that the catalyst gains further rooms for the oxygen activation to accelerate the CO oxidation; transition from CO-rich to O-rich regimes in a narrow T_s range.[25] The shift of the universal curve with P_{CO} indicates the higher T_s for the transition because of the higher frequency of the CO adsorption. At higher T_s, the thermal desorption of CO becomes more prominent to reduce the CO concentration (coverage) on the catalyst and hence results in the rate drop.

The apparent rate constant, k', of the CO oxidation was obtained by the following rate equation according to the Langmuir-Hinshelwood mechanism;[25]

$$\text{CO oxidation rate} = k' P_{O2} / P_{CO} \quad (2),$$

which has been confirmed at temperatures below that for a maximum rate.[25] The apparent rate constant thus obtained is plotted in Figure 4. The T_s dependence of k' is almost similar irrespective of P_{CO} at a given P_{O2}, and T_s shifts to higher at higher P_{O2}. The similarity indicates that the reaction mechanism does not change under the current reaction conditions. The T_s shift with P_{O2} (or the total pressure) is also consistent with the studies on single crystal suffaces.[25]

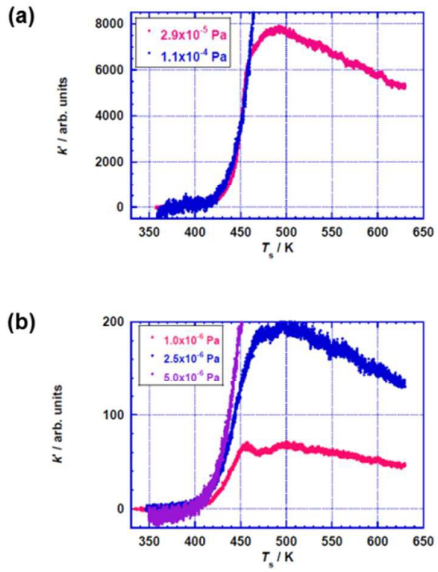

Fig. 4 Apparent rate constant, k', of the CO oxidation driven by the Pt_{30}/Si catalyst under steady-state reaction conditions at the partial pressure of O_2, (a) P_{O2}=1.0×10^{-4} Pa and (b) 2.5×10^{-6} Pa, and at various ones of ^{13}CO, P_{CO}, as indicated in the figure. The color for a given P_{CO} is the same as that shown in Figure 2.

At smaller P_{CO}/P_{O2}, the CO oxidation takes place even below 330 K. This result indicates that in spite of at this low T_s, the CO poisoning is incomplete as long as the catalytic cycle is rotating in balance of the CO adsorption and the CO removal by the CO oxidation. Breaking this balance is also critical with respect to the P_{CO}/P_{O2} ratio; the O-rich to CO-rich transition occurs in similar ranges of P_{CO}/P_{O2}=0.058–0.29 and 0.20–0.40 at P_{O2}=1.0×10^{-4} and 2.5×10^{-6} Pa, respectively. Anti-poisoning behaviour has been also reported in the CO oxidation by Pd clusters supported on MgO substrate.[28]

Conclusions

It appears that the Pt clusters directly bound to the Si substrate surface possess a particularly high catalytic performance in the CO oxidation; the low-temperature and anti-CO-poisoning performance. Considering that the reductive promotion of oxygen to an oxidizing agent is the critical in coexistence with CO, it is probable that this high performance originates from the accumulated electrons at the subnano-interface between the monatomic-layered Pt_{30} disk and the Si surface. Namely, the promotion of the cluster to the high-performance catalyst is achieved by the interaction with Si surface through both electronic and geometric aspects.

Acknowledgements

This research was supported by the Special Cluster Research Project of Genesis Research Institute, Inc. and JSPS Grant-in-Aid for Scientific Research (KAKENHI) (C) Grant Number 15K04594.

Notes and references

1 T. Bernhardt, U. Heiz and U. Landman, in *Nanocatalysis*, ed. U. Heiz and U. Landman, Springer, Berlin, 2007, Chapter 1, 1.
2 M. Haruta, *Faraday Discuss.*, 2011, **152**, 11.
3 A. Sanchez, S. Abbet, U. Heiz, W.-D. Schneider, H. Häkkinen, R. N. Branett and U. Landman, *J. Phys. Chem. A*, 1999, **103**, 9573.
4 B. Yoon, H. Häkkinen, U. Landman, A. S. Wörz, J.-M. Antonietti, S. Abbet, K. Judai and U. Heiz, *Science*, 2005, **307**, 403.
5 C. Zhang, B. Yoon and U. Landman, J. Am. Chem. Soc. 2007, 129, 2228–2229.
6 U. Heiz, F. Vanolli, A. Sanchez and W.-D. Schneider, *J. Am. Chem. Soc.*, 1998, **120**, 9668.
7 X. Lin, N. Nilius and H.-J. Freund, *Phys. Rev. Lett.*, 2009, **102**, 206801.
8 H. Yasumatsu, T. Hayakawa, S. Koizumi and T. Kondow, *J. Chem. Phys.*, 2005, **123**, 124709; *Virtual J. Nanoscale Sci. Technol.*, 2005.
9 H. Yasumatsu, T. Hayakawa and T. Kondow, *J. Chem. Phys.*, 2006, **124**, 014701.
10 H. Yasumatsu, T. Hayakawa and T. Kondow, *Chem. Phys. Lett.*, 2010, **487**, 279.
11 H. Yasumatsu, P. Murugan and Y. Kawazoe, *Phys. Stat. Solidi B*, 2012, **6**, 1193.
12 H. Yasumatsu and N. Fukui, *J. Phys. Chem. C*, 2015, **119**, 11217.
13 H. Yasumatsu and N. Fukui, *Phys. Chem. Chem. Phys.*, 2014, **16**, 26493.
14 H. Yasumatsu and N. Fukui, *Can. J. Chem. Eng.*, 2014, **92**, 1531.
15 H. Yasumatsu and N. Fukui, *Surf. Interface Anal.*, 2014, **46**, 1204.
16 K.-H. Allers, H. Pfnür, P. Feulner, D. Menzel, *J. Chem. Phys.*, 1994, **100**, 3985.
17 C. T. Campbell, G. Ertl, H. Kuipers and J. Segner, *J. Chem. Phys.*, 1980, **73**, 5862.
18 N. Fukui and H. Yasumatsu, *Euro. Phys. J. D*, 2013, **67**, 81.
19 H. Yasumatsu and T. Kondow, *Rep. Prog. Phys.*, 2003, **66**, 1783.
20 H. Yasumatsu and N. Fukui, *J. Phys. Conf. Ser.*, 2013, **438**, 012004.
21 H. Yasumatsu, *Euro. Phys. J. D*, 2011, **63**, 195.
22 H. Yasumatsu, M. Fuyuki, T. Hayakawa and T. Kondow, *J. Phys. Conf. Ser.*, 2009, **185**, 012057.
23 N. C. Flowers, N. B. Jonathan, Y. Liu and A. Morris, *J. Chem. Phys.*, 1995, **102**, 1034.
24 J. T. Miller, B. L. Meyers, F. S. Modica, G. S. Lane, M. Vaarkamp and D. C. Koningsberger, *J. Catal.*, 1993, **143**, 395.

25 T. Engel and G. Ertl, in *Adv. Catal.*, Academic Press, Inc., 1979, Volume 28, 1.
26 C. Henry, Chem. in *Chem. Phys. Solid Surf.*, Elsevier Science, 2003, Volume 11, 247.
27 F. Gao, S. M. McClure, Y. Cai, K. K. Gath, Y. Wang, M. S. Chen, Q. L. Guo and D. W. Goodman, *Surf. Sci.*, 2009, **603**, 65.
28 S. Kunz, F. F. Schweinberger, V. Habibpour, M. Röttgen, C. Harding, M. Arenz and U. Heiz, *J. Phys. Chem. C*, 2010, **114**, 1651.